Differentiating transmural from transanastomotic prosthetic graft endothelialization through an isolation loop-graft model

Timothy Pennel, MBChB, Peter Zilla, MD, PhD, and **Deon Bezuidenhout, PhD,** *Cape Town, South Africa*

Background: **In humans, transanastomotic endothelial outgrowth onto the surface of prosthetic vascular grafts is limited to the immediate perianastomotic region, even after years of implantation. In contrast, continual transanastomotic outgrowth together with short graft lengths has led to early endothelial confluence in most animal models pre-empting endothelialization through transmural capillary sprouting. We describe an isolation loop-graft model that clearly separates these distinctly different events.**

Methods: **Baseline transanastomotic endothelialization was assessed by implanting low-porosity expanded polytetrafluoroethylene grafts (ePTFE; internal diameter 1.7 mm; internodal distance 15-25 μm; 14.2 ± 1.6 mm long) for 2, 4, and 6 weeks (n = 6/time point) in the abdominal aorta of Wistar rats. High-porosity polyurethane (internal diameter 1.7 mm-150 μm pore size) grafts were then interposed ("welded") into the midsection of the ePTFE grafts for 2, 4, 6, and 8 weeks (n = 6/time point). Looping the interposition grafts increased their length to 70.3 ± 8.3 mm. After implantation periods of 6, 8, 12, and 24 weeks (n = 8/time point) isolation loop grafts were analyzed by light, immune-fluorescence (CD31) and scanning electron microscopy, and endothelialization was expressed as maximal transanastomotic endothelial outgrowth (I_{max}), mean transanastomotic outgrowth (I_{mean}), and segmental graft coverage (G_{SE}).**

Results: **Transanastomotic outgrowth slowed down between 2 and 6 weeks of implantation (proximal: [I_{max} from 0.9 ± 0.5 to 0.3 ± 0.3 mm/wk; $P < .04$; I_{mean} from 0.3 ± 0.1 to 0.2 ± 0.1 mm/wk; nonsignificant (NS)]; distal: [I_{max} from 0.7 ± 0.3 to 0.3 ± 0.2 mm/wk; $P < .02$; I_{mean} from 0.3 ± 0.2 to 0.2 ± 0.0 mm/wk; NS]) but remained constant thereafter (I_{max} = 0.5 ± 0.2 mm/wk; I_{mean} = 0.4 ± 0.2 mm/wk at 24 weeks NS). In straight composite grafts, the ePTFE separation zones were too short to isolate transmural ingrowth beyond week 4. In contrast, a broad endothelial-free separation zone was preserved in all looped composite grafts even after half a year of implantation (25.9 ± 5.9 vs 8.7 ± 4.9 mm proximally and 21.9 ± 13.4 vs 12.3 ± 6.2 mm distally at 6 and 24 weeks, respectively). Ninety-three percent of patent loop-grafts showed isolated transmural midgraft endothelium after 4 weeks and 97% after 6 weeks. Midgraft preconfluence was reached by 6 weeks (G_{SE} = 55 ± 45%) and confluence between week 12 and 24 (G_{SE} = 95.0 ± 10.0% and 84.0 ± 30.13%). The subintimal thickness stayed constant with a nonsignificant trend toward regression (91.8 ± 93.9 mm vs 71.4 ± 59.4 mm at 6 and 24 weeks, respectively; NS).**

Conclusions: **Transmural endothelialization can be clearly distinguished from transanastomotic outgrowth in a high throughput rat model. A looped interposition graft model provides sufficient isolation length to separate the two events for up to half a year and does not result in an increase in intimal hyperplasia. (J Vasc Surg 2013;58:1053-61.)**

Clinical Relevance: **Although the mode of graft deployment has changed over the years, the problem of an absent surface endothelium remains, whether small- to medium-diameter grafts are surgically implanted or placed endovascularly as "covered stents." In contrast to humans, most animal models experience progressive transanastomotic endothelial outgrowth. Together with graft lengths that were too short, the clinically irrelevant transanastomotic endothelialization inadvertently led to early endothelial confluence in the vast majority of experimental vascular graft studies pre-empting or concealing alternative modes of endothelialization. The isolation loop-graft model we propose allows the long-term differentiation of the different modes of endothelialization in a small animal screening model.**

From the Christian Barnard Department of Cardiothoracic Surgery, Cardiovascular Research Unit, University of Cape Town.

This work is based upon research supported by the National Research Foundation and the Medical Research Council of South Africa.

Author conflict of interest: none.

Reprint requests: Peter Zilla, MD, PhD, Christian Barnard Department of Cardiothoracic Surgery, Cardiovascular Research Unit, University of Cape Town, Faculty of Health Sciences, Cape Heart Center, Chris Barnard Building, Anzio Road, ZA 7925 Observatory, Cape Town, South Africa (e-mail: peter.zilla@uct.ac.za).

The editors and reviewers of this article have no relevant financial relationships to disclose per the JVS policy that requires reviewers to decline review of any manuscript for which they may have a conflict of interest.

0741-5214/$36.00

http://dx.doi.org/10.1016/j.jvs.2012.11.093

Synthetic small- to medium-sized vascular grafts have inherent shortcomings regardless of whether they are surgically implanted or endovascularly placed as "covered stents." One such shortcoming is the lack of an endothelial lining even after years of clinical implantation. This absence of a physiological intima is a main reason for lower patency rates compared with arterial or vein grafts.[1]

Although sophisticated surface coatings with carbon[2]; heparin[3,4]; polypropylene-sulfide-polyethylene glycol[5]; thrombomodulin[4]; acrylate-phospholipid[6] or elastin polymers,[7] or the release of thromboinhibitory molecules such as nitric oxide[8] have been partially successful in improving graft performance, a functional endothelium remains the most desirable nonthrombogenic surface.[1,9]

The most natural mode of achieving an endothelial lining on synthetic grafts would be transanastomotic outgrowth from adjacent arteries. However, for reasons incompletely understood, transanastomotic endothelialization in humans does not reach further than the immediate perianastomotic region even after decades of implantation.[10] Together with graft lengths of up to 50 to 60 cm, it is evident that endothelialization strategies that hinge on transanastomotic outgrowth are futile in man. Yet, 40 years of vascular graft research have counterintuitively and often unintentionally focused on transanastomotic endothelialization.[1] By choosing short graft lengths in animal models that lack the transanastomotic outgrowth stoppage of humans, most experimental prostheses were transanastomotically fully endothelialized at the time of explantation making it impossible to assess any other mode of endothelialization. In over 90% of large animal studies performed over almost 4 decades, the average graft length was 5.5 cm in Dacron and expanded polytetrafluoroethylene (ePTFE) grafts and even shorter in polyurethane (PU) grafts.[1] Although slightly longer grafts have been implanted in more recent years (two-thirds are still shorter than 7 cm), the endothelialization observed was still largely due to the vigorous transanastomotic outgrowth intrinsic to the animal models used. The same outgrowth distance, for instance, which takes 56 weeks in humans to be covered is reached after 3.5 weeks in dogs.[1] Furthermore, apart from the differences between species, senescence also needs to be considered. As an example, senescent baboons come closest to the situation in man, yet the transanastomotic endothelialization in senescent dogs is comparable to that in juvenile baboons.[1] To further complicate the issue, anatomic dimensions of species play a role, as it is impossible to directly compare outgrowth distances in rats with those in large animals.[1] Yet, if expressed in relative terms, juvenile large and small animals have comparable transanastomotic outgrowth rates. Both rats and sheep, for instance, cover a distance equivalent to the inner diameter of the infrarenal aorta within a month.[1]

Given the fact that transanastomotic endothelialization is not only irrelevant in humans but also highly variable in animals, experimental models that are capable of investigating alternative modes of endothelialization without transanastomotic interference are critically needed. The three alternative modes of endothelialization that such models theoretically need to allow to study in isolation are transmural capillary sprouting, fallout healing from the blood stream, and the transplantation of autologous endothelial cells onto or into the scaffold of a synthetic graft.

The latter approach represented the first broad manifestation of tissue engineering in the late 1970s and 1980s. Although its single-stage variant resulted in too low an inoculum under clinical conditions,[11,12] the two-stage approach utilizing cell culture techniques[13,14] served as a proof of superiority of endothelialized synthetic vascular grafts.[15,16] However, inasmuch as tissue engineering approaches such as in vitro endothelialization were able to close the gap between prosthetic and autologous grafts,[15,16] their demand for a high level of methodological sophistication makes them an unrealistic solution for the many thousands of synthetic vascular grafts annually implanted in patients.

To investigate whether transmural ingrowth or fallout healing could hold a realistic key to spontaneous in vivo endothelialization, animal models are critically required to clearly separate these events from transanastomotic outgrowth. A similar need exists to separate transanastomotic intimal hyperplasia (often referred to as *pannus outgrowth*) from independently developing subendothelial tissue. While transanastomotic intimal hyperplasia is a major contributor to prosthetic graft failure, subintimal tissue in the midgraft region may either be flow-controlled and as such, self-limiting or lumen encroaching like its anastomotic counterpart.

We have previously proposed a model that isolates a high-porosity midsegment from transanastomotic outgrowth through sufficiently long proximal and distal low-porosity segments.[1] In the present study, we realized this concept in a high-throughput small animal model allowing adequate isolation lengths through looping of the graft.

METHODS

Study design. An infrarenal aortic interposition model was chosen in male Wistar rats (449 ± 50 g). Fourteen millimeter long (14.2 ± 1.6 mm) straight low-porosity ePTFE grafts (n = 18/6 per group) were implanted and explanted over increasing time intervals (2; 4; 6 weeks) to assess transanastomotic endothelialization. Subsequently, straight ePTFE grafts of equal length had 4-mm-long high-porosity PU segments centrally inserted (total length, 18.4 ± 1.5 mm) to determine the time point from which onward transmural and transanastomotic endothelialization become indistinguishable (n = 24/6 per group; implantation period 2, 4, 6, and 8 weeks). Finally, loop grafts (implantation length 70.3 ± 8.3 mm; n = 32/8 per group) with a high-porosity PU segment in the midsection were implanted allowing a manifold length extension of the isolating low-porosity ePTFE segments and thereby ensuring clearly discernible endothelial free zones over implantation periods of up to half a year (6, 8, 12, and 24 weeks) (Fig 1). To exclude the possibility of transmural endothelialization occurring through gaps at the interface between midgraft and the ePTFE isolation segments, control composite grafts were implanted where the interposition segment also consisted of low-porosity ePTFE.

Vascular grafts. Low-porosity ePTFE grafts (Zeus Industrial Products Inc, Orangeburg, SC) (internal diameter [ID]:1.77 ± 0.05 mm; outer diameter [OD]:2.48 ± 0.05 mm; internodal distance [IND]:15-25 μm) without external wrap were used throughout. The high-porosity PU (Medtronic Inc, Minneapolis, Minn) midgraft segments were manufactured as previously described[1,17,18] using spherical gelatin beads (Thies Technologies, St. Louis, Mo) to create well-defined interconnected ingrowth spaces (pore size, 156 ± 2 μm with 76 ± 2 μm interconnections). Midgraft segments were "welded" to the two ePTFE segments with 10% PU chloroform. The looped grafts (manufacturing length, 90 mm; loop diameter, 15 mm; PU

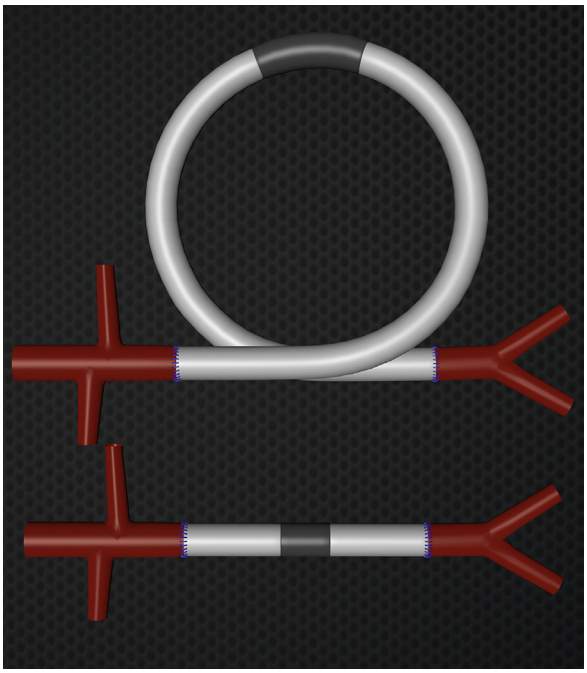

Fig 1. Straight and loop grafts are interpositioned between the renal arteries and the aortic bifurcation of Wistar rats. An 8-mm-long high-porosity (pore size, 156 μm; minimal interconnecting pore size, 76 μm) polyurethane graft segment (*gray*) is "welded" into the midpart of a low-porosity expanded polytetrafluoroethylene (ePTFE) graft (internodal distance [IND] 15-25 μm) (*white*). As the midgraft segment is ingrowth permissible for transmural capillaries and arterioles, whereas the "isolation arms" on each side are impenetrable for blood vessels, transmural endothelialization can be investigated without interference by transanastomotic endothelialization. Looping the graft increased the isolation length, ensuring an endothelial-free zone.

interposition segment, 8 mm) were identically manufactured but heat-set in 75°C water for 3 minutes over a spiraled 1.5-mm nylon cord that preserved the loop shape without kinking. Every 10th graft was excluded from implantation for quality control analyses.

Surgery. All animal experiments were approved by the Animal Research and Ethics Committee of the University of Cape Town and were in compliance with the Guide for the Care and Use of Laboratory Animals, Institute of Laboratory Animal Resources, Commission on Life Sciences, National Research Council. Operations were performed under general anesthesia (isoflurane 1.75% nosecone) and under sterile conditions in spontaneously breathing animals. After a midline laparotomy, the high-porosity PU segment was pre-clotted with venous blood following which the infrarenal aorta was mobilized and heparin was administered (1 mg/kg) prior to aortic cross-clamping. The abdominal aorta was transected in a beveled manner and grafts were anastomosed with interrupted 9-0 nylon (Ethilon; Johnson & Johnson, New Brunswick, NJ) using an operation microscope (Zeiss Universal S3, Oberkochen, Germany). The cross-clamp time did not differ between the straight (44.1 ± 10.6 minutes) and looped groups (42.7 ± 8.3 minutes; nonsignificant [NS]). If grafts continued to ooze following clamp removal, the aorta was clamped and unclamped for 1 minute in an intermittent fashion until the hemostasis was achieved. The looped grafts were secured to the lumbar muscles to prevent twisting. All grafts were covered by the retroperitoneum. Prior to closure, buprenorphine (0.1 mg/kg) was administered subcutaneously. Animals were kept in temperature-controlled rooms with a 12-hour light/dark cycle and fed ad libitum. Initially, they were kept in separate cages during their first 3 days postoperatively receiving twice-daily subcutaneous analgesia (buprenorphine 0.1 mg/kg), following which they were paired for social interaction. At the end of the implantation period, rats were euthanized under isoflurane anesthesia and retroperitoneal tissue incorporation was confirmed (Fig 2). After the distal aorta had been inspected for patency, 1 mg/kg heparin was administered via the inferior vena cava prior to the animal being sacrificed by exsanguination. On apnea, the chest was opened and a 22-gauge cannula was transapically advanced into the ascending aorta. Phosphate-buffered solution (37°C) was perfused first until clear fluid drained out the transected right atrium (minimum of 200 mL) followed by 150 mL of 1% paraformaldehyde perfusion-fixation. Vascular graft angiography (Philips BV Pulsera; Philips, Amsterdam, The Netherlands) was performed with 10 mL nonionic contrast medium (Omnipaque 300; GE Healthcare, Little Chalfont, United Kingdom) (Fig 3). The graft was then explanted en bloc.

Histologic and scanning electron microscopy (SEM) analyses of endothelialization and tissue incorporation. Following macrophotography and excision of 2-mm-long midgraft cross-sections, all grafts were divided longitudinally for histologic and SEM analysis except for two loop grafts per group that were exclusively used for histologic serial sections. SEM specimens were postfixed in glutaraldehyde (2.5%; 0.1 M/L phosphate buffer; 24 hours; 4°C), dehydrated in graded ethanol, critical point dried (Polaron, Evanstone, Ill), sputter coated, and analyzed in a Jeol JSM 5200 using Image J v1.41 (National Institute of Health, Bethesda, Md) image analysis software. Maximal transanastomotic endothelial outgrowth distance (I_{max}) was perpendicularly measured from the anastomoses to the tip of the furthest reaching endothelial "tongue" (Fig 4). The mean transanastomotic outgrowth (I_{mean}) defined as the area of the endothelialized region divided by the average width (w) of the sample, can be written in terms of the areas A_1, A_2 and I_{max} as shown below:

$$(A_1 + A_2) = I_{max} \times w$$
$$A_1 = I_{mean} \times w$$
$$I_{mean} = \left(\frac{A_1}{A_1 + A_2}\right) \times I_{max}$$

Overall graft endothelialization (G_E) was expressed as percentage of endothelial covered surface of an entire graft, whereas (GS_E) refers to endothelialization of a graft

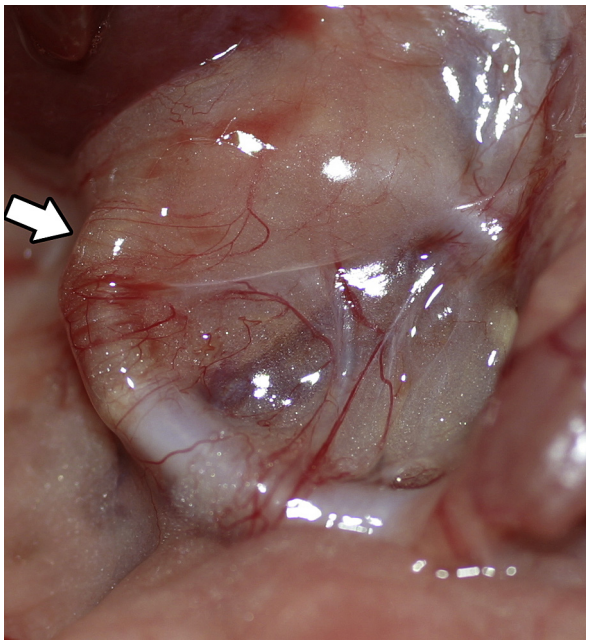

Fig 2. Isolation loop graft at explantation. While one can still recognize the high-porosity midgraft segment after 12 weeks of implantation (*arrow*), the entire loop has been well incorporated into retroperitoneal tissue.

segment (ePTFE or PU). Endothelial-free zones were defined as the minimum distance between the furthest reaching points of opposing transanastomotic endothelial outgrowth. Samples for histology were postfixed in zinc solution (24 hours; 4°C), embedded in paraffin, and stained with hematoxylin (Merck, Damstadt, Germany) and eosin (BDH; WWR International, Poole, England) (H&E), Miller and Masson elastin trichrom stain, anti-CD31 (Fitzgerald International, North Acton, Mass), anti-factor VIII von Willebrand (Dako, AS, Glostrup, Denmark) antibodies for immune histochemistry to label endothelial cells, and anti-alpha actin (Abcam, Cambridge, UK) antibodies to label smooth muscle cells. Slides were viewed under a Nikon eclipse 90i microscope (Nikon, Tokyo, Japan). The histologic presence of surface endothelium was cross-referenced against the SEM analysis to confirm interpretation. Neo-intimal hyperplasia was defined as the tissue layer between the graft and the blood surface excluding thrombus appositions.

Statistical analysis. Statistical tests were performed with STATA (StataCorp 2011, Stata Statistical Software: Release 12; StataCorp LP, College Station, Tex) Results were expressed as mean ± SD for continuous variables. The unpaired *t*-test was used to compare normally distributed data and Mann-Whitney for nonparametric values. The level of significance was set at $P < .05$.

RESULTS

Overall graft patencies were 100% (18/18) for straight ePTFE grafts, 100% for straight ePTFE/ePTFE composite-graft controls, 92% for straight ePTFE/PU composite grafts (22/24), and 84% (27/32) for looped ePTFE/PU composite grafts (mean implantation time 28 ± 11.7 days; 28 ± 0 days; 35 ± 15.9 days; and 87.5 ± 49.7 days, respectively).

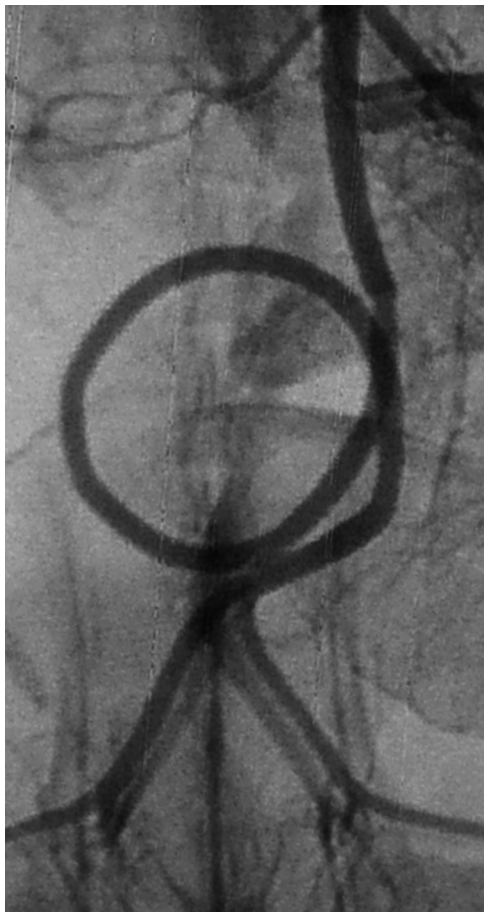

Fig 3. Angiogram depicting the loop graft in situ taken immediately after euthanasia. After 24 weeks of implantation, the looped graft appears undistorted and without any kinks. No signs of midgraft narrowing suggest lumen-encroaching subintimal tissue formation.

From week 2, all grafts showed zones of smooth, glistening blood surfaces stretching across both aortic anastomoses and expanding with increasing implantation time. From week 4 onward, similar tissue began to emerge on the midgraft PU sections.

Transanastomotic endothelial outgrowth

ePTFE grafts (straight). After 6 weeks, there was no significant difference between proximal and distal outgrowth (I_{max} = 2.9 ± 1.4 vs 2.1 ± 0.6 mm; NS/I_{mean} = 0.9 ± 0.8 vs 1.1 ± 0.3; NS). Indexed over time, transanastomotic outgrowth slowed down between 2 and 6 weeks of implantation (proximal: I_{max} from 0.9 ± 0.5 to 0.3 ± 0.3 mm/wk; $P < .04$/I_{mean} = 0.3 ± 0.1 vs 0.2 ±

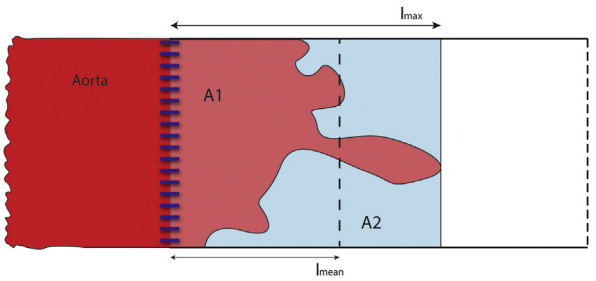

Fig 4. Maximal transanastomotic endothelial outgrowth distance (I_{max}) was perpendicularly measured from the anastomoses to the tip of the furthest-reaching endothelial "tongue." The mean transanastomotic ingrowth (I_{mean}) defined as the area of the endothelialized region divided by the average width (w) of the sample, can be written in terms of the areas A_1, A_2, and I_{max} as follows:

$$(A_1 + A_2) = I_{max} \times w$$
$$A_1 = I_{mean} \times w$$
$$I_{mean} = \left(\frac{A_1}{A_1 + A_2}\right) \times I_{max}$$

0.1; NS; distal: I_{max} from 0.7 ± 0.3 to 0.3 ± 0.2 mm/week; $P < .02$/I_{mean}= 0.3 ± 0.2 vs 0.2 ± 0.0; NS). Total graft endothelialization was G_E = 10.0 ± 6.3%; 18.7 ± 11.3% and 40.0 ± 35.1% at 2, 4, and 6 weeks, respectively.

ePTFE/PU composite grafts (straight). As early as from week 4 onward, bilateral transanastomotic outgrowth from both the aorta and the porous central PU segment led to endothelial continuity in one-third of grafts making it impossible to distinguish between transanastomotic and transmural origin. From week 6 onward, all grafts showed uninterrupted endothelial continuity (Figs 5 and 6, *A*). The overall endothelial coverage of the entire graft was G_E = 10.0 ± 0.0; 37.2 ± 17.0; 70.0 ± 12.2 and 73.3 ± 12.5% at 2, 4, 6, and 8 weeks.

ePTFE/PU composite grafts (looped). After 24 weeks, transanastomotic endothelialization reached 10.9 ± 3.1 mm (I_{max})/9.3 ± 3.4 mm (I_{mean}) from the aorta onto the proximal ePTFE segment of the loop and 14.1 ± 7.1 mm (I_{max})/10.9 ± 5.3 mm (I_{mean}) onto the distal one. There was no significant difference between proximal and distal outgrowth. Over the entire observation period of looped composite grafts, transanastomotic endothelial outgrowth remained constant (I_{max} = 0.7 ± 0.9 mm/wk /I_{mean} = 0.5 ± 0.6 mm/wk at 6 weeks vs I_{max} = 0.5 ± 0.2 mm/wk / I_{mean} = 0.4 ± 0.2 mm/wk at 24 weeks NS).

Endothelial outgrowth from the high-porosity central PU segment onto the isolating ePTFE segments was first detectable at week 2. Until 24 weeks, it reached 5.4 ± 6.7 mm (I_{max})/3.8 ± 4.2 mm (I_{mean}) onto the proximal ePTFE segment and 3.8 ± 4.0 mm (I_{max})/1.7 ± 1.9 mm (I_{mean}) onto the distal one (Fig 7).

At all time points, 100% of grafts maintained an endothelial-free zone between the transanastomotic and the transmural endothelium. Between week 6 and 24, the endothelial-free zone decreased from 25.9 ± 5.9 to 8.7 ± 4.9 mm proximally and 21.9 ± 13.4 to 12.3 ± 6.2 mm distally (Fig 6, *B*).

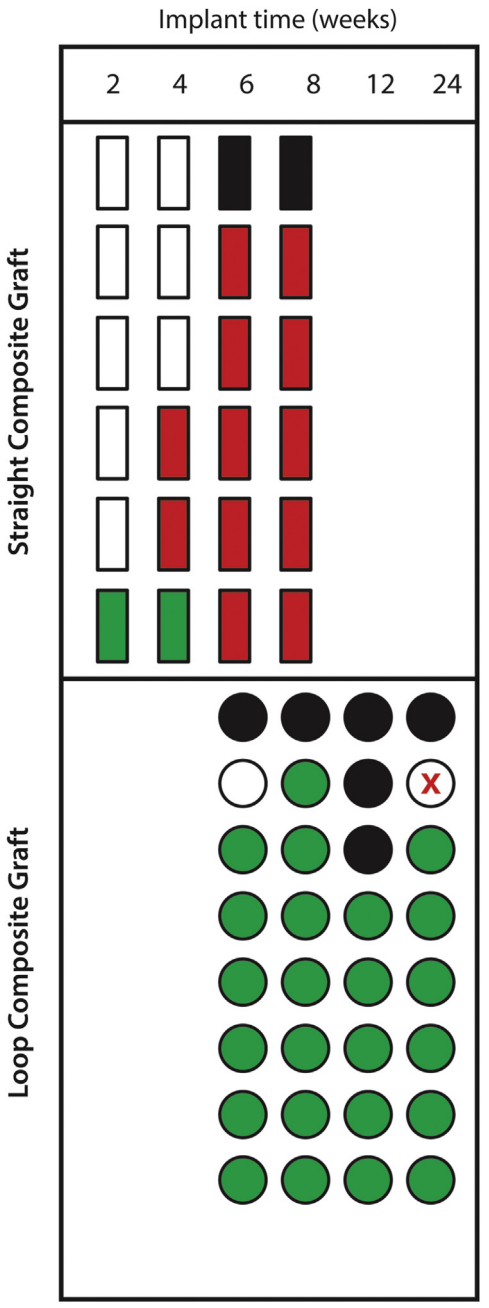

Fig 5. Compilation of individual straight (*rectangles*) and looped (*circles*) composite grafts in relation to the isolation of midgraft endothelium. *Green* indicates those grafts where clear endothelial-free zones were present between midgraft and transanastomotic endothelium, whereas *red* indicated a coalescence of the two across the entire graft length. It is obvious that from week 2 onward, isolation begins to disappear in the shorter straight grafts (*no filling*, absent midgraft endothelium; *X*, loop graft remained nonembedded; *black*, occluded graft).

Midgraft endothelialization

ePTFE | ePTFE composite control grafts (straight). Prior to the advancing transanastomotic endothelium

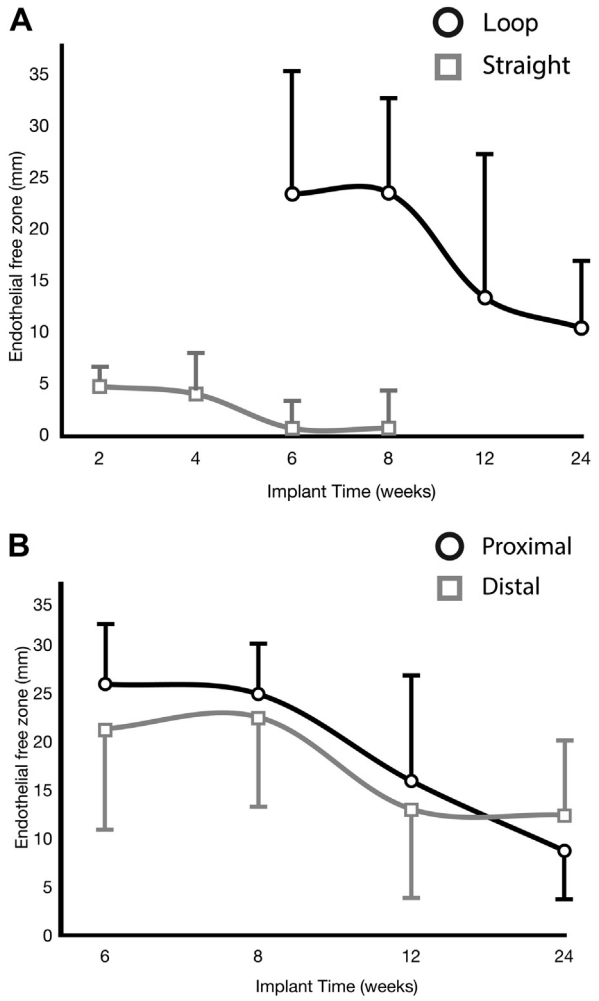

Fig 6. Endothelium-free zones on the low-porosity expanded polytetrafluoroethylene (ePTFE) isolation segments. **A,** It is obvious that, in contrast to straight composite grafts, the endothelial-free zones in the loop grafts are sufficiently wide to allow even longer implantation periods than 6 months. **B,** Between week 6 and 24, there is no difference in the proximal and distal endothelial-free zones.

leading to complete endothelial confluence, none of the ePTFE control grafts (neither ePTFE-only nor ePTFE/ePTFE composite grafts) showed any signs of midgraft endothelium at any time point.

ePTFE/PU composite grafts (straight). Only one (17%) of the 2-week composite grafts showed traces of endothelium on the midgraft covering 7.3% (GS_E 1.6 ± 4.1%) of the PU surface as opposed to four (67%) of the 4-week explants that showed evidence of midgraft endothelium (GS_E = 50.0 ± 43.8%) (Fig 8). All of the 6- and 8-week samples had preconfluent to confluent endothelium on the high-porosity midgraft segment (GS_E = 94.0 ± 1348% and 90.0 ± 14.1%, respectively).

ePTFE/PU composite grafts (looped). Except for one 6-week graft and one 24-week graft, all loop grafts showed the presence of endothelium on the PU segment from week 6 onward. The nonendothelialized 24-week graft had failed to embed in the retroperitoneum and as such remained free-floating in the abdomen. In the absence of any connection to surrounding tissue and a complete lack of transmural capillaries, this graft was excluded from the analysis. In the remaining 30/32 grafts, endothelial coverage of the midgraft PU segment was 72.0 ± 42.1%; 91.7 ± 11.7%; 95.0 ± 10.0% and 84.0 ± 30.13% at 6, 8, 12, and 24 weeks, respectively (Fig 8).

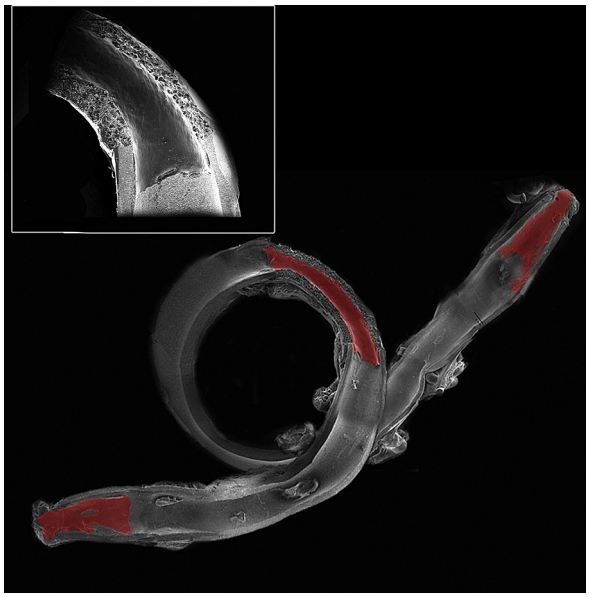

Fig 7. Stitched composite picture of the standard error of the mean images used to analyze surface endothelialization. The endothelialized areas were marked in red. The *insert* shows how the transmural midgraft endothelium eventually also begins to grow across the anastomotic seam line with the expanded polytetrafluoroethylene (ePTFE) graft additionally narrowing the endothelial-free zone from the midgraft side.

Transmural vessel ingrowth. Apart from the one excluded 24-week graft, all patent composite grafts showed radial CD31-positive capillary ingrowth or endothelial cells sprouting without a lumen into the PU segments from the outside toward the blood surface. As early as at 2 weeks, transmural vessel ingrowth reached the inner third of the graft wall in all implants while CD31-positive cells remained scanty in the vicinity of the blood surface (Fig 9).

Intimal hyperplasia. The subintimal tissue on the midgraft segment showed varying degrees of cellularity and collagen content. Once a full endothelium was established at 6 weeks, the subintimal thickness stayed constant with a nonsignificant trend toward regression (91.8 ± 93.9 mm vs 71.4 ± 59.4 mm at 6 and 24 weeks, respectively; NS).

DISCUSSION

After decades of animal experiments that mostly failed to distinguish between transanastomotic and transmural

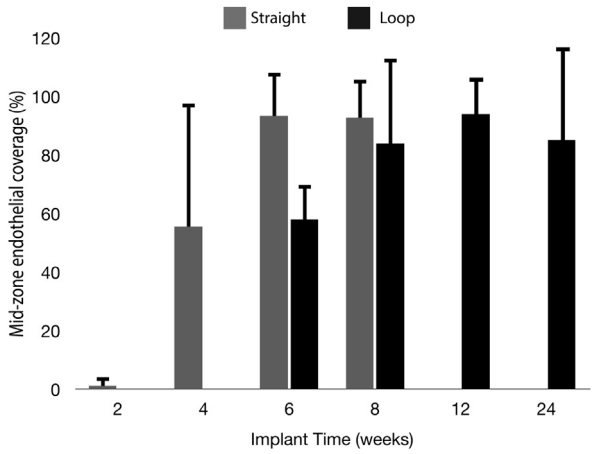

Fig 8. Percentage of endothelial coverage of the high-porosity midsection of composite grafts. The fact that the short, straight composite grafts (*gray*) showed faster midgraft endothelialization than the isolation loop grafts (*black*) highlights the likelihood of transanastomotic outgrowth reaching the midgraft early in the absence of sufficiently long "separation" distances.

endothelialization, we were able to clearly separate the two events in an infrarenal isolation model in the rat. By implanting composite prostheses consisting of a high-porosity midsegment welded into a low-porosity ePTFE graft, we could demonstrate the following:

- In straight composite grafts, isolation segments were too short making it impossible to distinguish between transanastomotic and transmural endothelium.
- By extending the low-porosity isolation segments through looping, broad endothelial-free zones were maintained on either side of the midgraft in 100% of implants even after half a year of implantation.
- From 6 weeks, transmural midgraft endothelium was present in 93% of loop implants.
- Except for the initial 2 weeks, transanastomotic endothelialization onto low-porosity ePTFE occurred at a constant average speed of 0.3 to 0.4 mm/wk and a maximal speed of 0.3 to 0.5 mm/wk.
- Subintimal tissue formation on midgrafts was modest and did not progress once endothelial confluence was reached.

Given the continual presence of broad endothelial-free separation zones in all loop grafts after half a year of implantation, our rat model has allowed us, for the first time, to precisely assess modes of endothelialization other than transanastomotic.

Notwithstanding, as the rat has always been a preferred small animal screening model, it was extensively used in vascular graft research in the past in spite of limited length of suitable arteries. As a consequence, far too short grafts of 10- to 15-mm length were implanted.[19-25] If one conservatively extrapolates the transanastomotic outgrowth rates in rats,[22,25,26] it is highly likely that these experimental grafts

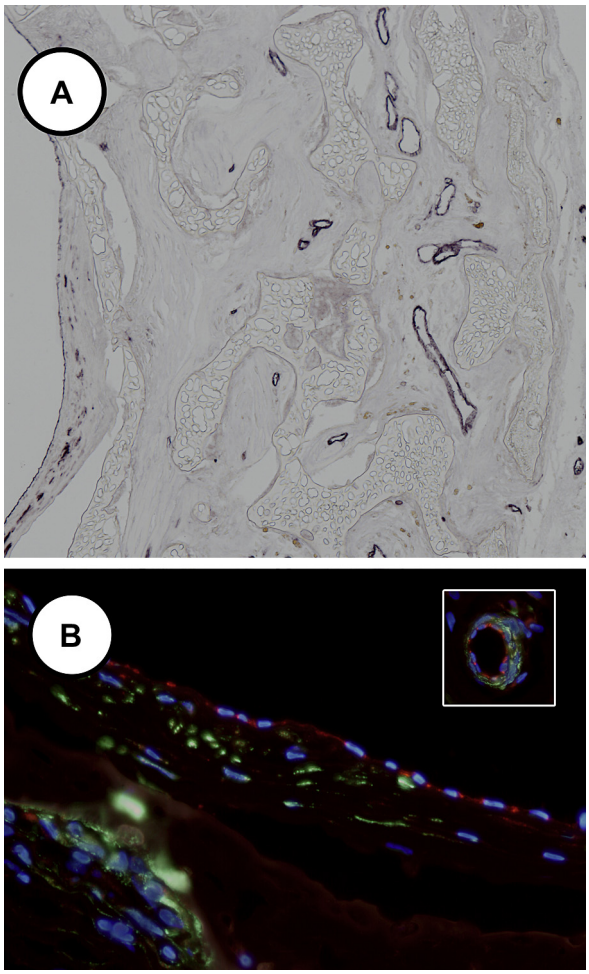

Fig 9. Immunohistochemistry of the high-porosity polyurethane (PU) midgraft segment of loop implants (12-week implants) and scanning electron microscopy (SEM) of anastomosis. **A,** CD31-positive endothelial cells cover the blood surface and are seen as intramural vessels as well as single-stranded endothelial sprouts (×10). **B,** Neointima with confluent endothelium on top of a modest layer of alpha-actin-positive smooth muscle cells. (*Insert*: ×40) The large interconnecting pore sizes of ≥76 μm enable arteriole ingrowth deep into the interstices of the graft wall (×40). **C,** SEM image depicting transanastomotic endothelialization of expanded polytetrafluoroethylene (ePTFE) isolation segment (×15)

were all transanastomotically fully endothelialized within less than 10 weeks. Given the individual variability of transanastomotic outgrowth, transanastomotic confluence needs to be assumed even earlier. In recognition of this shortcoming, some researchers have emphasized the need for additional graft length. As early as in 1984, Hess et al[27] suggested a looped conduit that enables the implantation of graft lengths of up to 10 cm in the infrarenal aorta of the rat. However, while loop grafts allowed longer observation periods of transanastomotic outgrowth in low-porosity ePTFE grafts,[28] in high-porosity grafts the line between transanastomotic and transmural

endothelialization continued to be blurred.[29] As these prostheses permit transmural ingrowth across the entire length of the grafts, transmural vessels could theoretically contribute to the surface endothelium anywhere on the graft including the proximity of the anastomoses. Conversely, transanastomotic outgrowth has been described to occur significantly faster on high-porosity grafts[22,25] increasing the likelihood of endothelium to be transanastomotic in origin even at considerable distance from the anastomoses.

Therefore, as the transition zone where the two modes of endothelialization coexist remained poorly defined, extending the graft length by looping did not result in a model that allowed the assessment of transmural events without transanastomotic interference. In view of the insignificance of transanastomotic endothelialization in clinically implanted grafts, a model was therefore needed that guarantees clearly discernible endothelial-free zones on either side of a high-porosity graft. By "welding" a short high-porosity segment into the center of a low-porosity graft, a separation of events was achieved. However, as the transmurally formed midgraft endothelium eventually began to also grow onto the low-porosity isolation segments, the endothelium-free separation zone disappeared rapidly in straight infrarenal interposition grafts because of their anatomic length limitation. By week 4, the two outgrowth margins had coalesced in 50% of implants and from week 6 onward, none of the straight composite grafts allowed the distinction between midgraft and transanastomotic endothelium any longer. Carrying the isolation principle over into loop grafts substantially increased the length of the isolation segments thereby guaranteeing a distinct endothelial-free separation zone that allowed the observation of transmural endothelialization without transanastomotic interference for up to half a year. Extrapolating the relatively constant mid- to long-term transanastomotic outgrowth rate of the present study of 0.2 to 0.3 mm/wk, it is likely that the isolation loop model will maintain a discernible endothelium-free isolation zone for up to a year. The fact that the outgrowth rate corresponds with previous observations[25,30] confirms the reproducibility of the model.

Isolated from transanastomotic endothelialization by endothelial-free zones, the high-porosity midgrafts experienced abundant vessel ingrowth from the surrounding tissue in 31 of 32 rats. In 50% of implanted loop grafts, transmural blood vessels reached the blood surface as early as after 2 weeks, comparable to juvenile baboons[31] but earlier than in dogs[32] or senescent baboons.[1] Only one graft failed to embed in the retroperitoneal tissue and remained freely floating in the abdomen. On gross examination, the porous midsegment was covered by a white smooth capsule. On histology, smooth muscle cells, macrophages, and collagen were present in the pores of the graft in the absence of even traces of an endothelium. Although this observation supports Julie Campbell's[33] finding that peritoneal macrophages are capable of transdifferentiating into fibroblasts and vascular smooth muscle cells, it puts the significance of "fallout" healing into perspective. Although described by Lester Sauvage's group[34] and Shi et al[35] as a possible source of midgraft endothelialization, the absolute lack of any traces of endothelium in the absence of transmural capillary ingrowth in the present study suggests that in this model, the main source of midgraft endothelium is transmural capillary ingrowth rather than bloodborne endothelial or progenitor cells. However, to firmly exclude the possibility of "fallout" healing, isolation loop-graft experiments will be required where the central high-porosity segment is sealed inside a low-porosity wrap of a pore size small enough to prevent capillary ingrowth but sufficiently porous to avoid the dismal occlusion rates of nonporous small-diameter grafts. Alternatively, distal arteriovenous fistulae have led to at least some degree of patency in impervious grafts that were sealed with silicone on their outside.[34] The presence of small endothelial islands after 3 months of implantation in dogs confirmed[34] the principal possibility of blood-derived fallout healing, while excluding it as a predominant mode of endothelialization. Similarly, small traces of endothelial islands were occasionally detectable on low-porosity woven Dacron prostheses in humans after prolonged implantation periods.[36] Overall, however, the observation of fallout healing has been scanty and so far limited to Dacron surfaces.[34-36]

In summary, we established a small animal vascular model that allowed us to study transmural endothelialization in isolation without the distorting presence of a preexisting transanastomotic endothelium. This also allowed us to address two concerns potentially jeopardizing its ultimate clinical success. One of these concerns is the fear that concomitant neointimal tissue proliferation may not be self-limiting. Although previous experiments have consistently shown a rapid appeasement of subintimal mitotic activity over time both in the rat[22,37] and in the baboon model,[38,39] one could argue that accelerated endothelial confluence because of transanastomotic contribution may have mitigated the process. The modest neointimal response we saw in the present study and its trend toward regression over time, however, confirmed the self-limiting nature of neointimal proliferation in isolated midgrafts.

The other concern relates to the suspected adverse build-up of increasingly hostile and impenetrable fibrin in the innermost graft layer[1,40] before transmural vessel ingrowth can reach the blood surface. The goal will be to accelerate capillary ingrowth[41] or to prevent the gradual compaction of fibrin. For both, a small animal model will be needed that allows the investigation of these processes over extended periods of time without the interference of transanastomotic endothelium.

AUTHOR CONTRIBUTIONS

Conception and design: PZ, DB
Analysis and interpretation: TP, DB, PZ
Data collection: TP
Writing the article: PZ, TP, DB
Critical revision of the article: PZ, DB, TP

Final approval of the article: PZ
Statistical analysis: TP, DB
Obtained funding: DB, PZ
Overall responsibility: PZ

REFERENCES

1. Zilla P, Bezuidenhout D, Human P. Prosthetic vascular grafts: wrong models, wrong questions and no healing. Biomaterials 2007;28:5009-27.
2. Kapfer X, Meichelboeck W, Groegler FM. Comparison of carbon-impregnated and standard ePTFE prostheses in extra-anatomical anterior tibial artery bypass: a prospective randomized multicenter study. Eur J Vasc Endovasc Surg 2006;32:155-68.
3. Bosiers M, Deloose K, Verbist J, Schroe H, Lauwers G, Lansink W, et al. Heparin-bonded expanded polytetrafluoroethylene vascular graft for femoropopliteal and femorocrural bypass grafting: 1-year results. J Vasc Surg 2006;43:313-8; discussion: 318-9.
4. Tseng PY, Rele SS, Sun XL, Chaikof EL. Membrane-mimetic films containing thrombomodulin and heparin inhibit tissue factor-induced thrombin generation in a flow model. Biomaterials 2006;27:2637-50.
5. Karrer L, Duwe J, Zisch AH, Khabiri E, Cikirikcioglu M, Napoli A, et al. PPS-PEG surface coating to reduce thrombogenicity of small diameter ePTFE vascular grafts. Int J Artif Organs 2005;28:993-1002.
6. Jordan SW, Faucher KM, Caves JM, Apkarian RP, Rele SS, Sun XL, et al. Fabrication of a phospholipid membrane-mimetic film on the luminal surface of an ePTFE vascular graft. Biomaterials 2006;27:3473-81.
7. Jordan SW, Haller CA, Sallach RE, Apkarian RP, Hanson SR, Chaikof EL. The effect of a recombinant elastin-mimetic coating of an ePTFE prosthesis on acute thrombogenicity in a baboon arteriovenous shunt. Biomaterials 2007;28:1191-7.
8. Smith DJ, Chakravarthy D, Pulfer S, Simmons ML, Hrabie JA, Citro ML, et al. Nitric oxide-releasing polymers containing the [N(O) NO]- group. J Med Chem 1996;39:1148-56.
9. Chlupac J, Filova E, Bacakova L. Blood vessel replacement: 50 years of development and tissue engineering paradigms in vascular surgery. Physiol Res 2009;58(Suppl 2):S119-39.
10. Berger K, Sauvage L, Rao A, Wood S. Healing of arterial prostheses in man: its incompleteness. Ann Surg 1972;175:118-27.
11. Herring M, Smith J, Dalsing M, Glover J, Compton R, Etchberger K, et al. Endothelial seeding of polytetrafluoroethylene femoral popliteal bypasses: the failure of low-density seeding to improve patency. J Vasc Surg 1994;20:650-5.
12. Zilla P, Fasol R, Deutsch M, Fischlein T, Minar E, Hammerle A, et al. Endothelial cell seeding of polytetrafluoroethylene vascular grafts in humans: a preliminary report. J Vasc Surg 1987;6:535-41.
13. Zilla P, Fasol R, Preiss P, Kadletz M, Deutsch M, Schima H, et al. Use of fibrin glue as a substrate for in vitro endothelialization of PTFE vascular grafts. Surgery 1989;105:515-22.
14. Zilla P, Preiss P, Groscurth P, Rosemeier F, Deutsch M, Odell J, et al. In vitro-lined endothelium: initial integrity and ultrastructural events. Surgery 1994;116:524-34.
15. Zilla P, Deutsch M, Meinhart J, Puschmann R, Eberl T, Minar E, et al. Clinical in vitro endothelialization of femoropopliteal bypass grafts: an actuarial follow-up over three years. J Vasc Surg 1994;19:540-8.
16. Deutsch M, Meinhart J, Zilla P, Howanietz N, Gorlitzer M, Froeschl A, et al. Long-term experience in autologous in vitro endothelialization of infrainguinal ePTFE grafts. J Vasc Surg 2009;49: 352-62; discussion: 362.
17. Bezuidenhout D, Davies N, Zilla P. Effect of well-defined dodecahedral porosity on inflammation and angiogenesis. ASAIO J 2002;48:465-71.
18. Schmidt C, Bezuidenhout D, Beck M, Van der Merwe E, Zilla P, Davies N. Rapid three-dimensional quantification of VEGF-induced scaffold neovascularisation by microcomputed tomography. Biomaterials 2009;30:5959-68.
19. van der Lei B, Wildevuur C. Microvascular polytetrafluoroethylene prostheses: the cellular events of healing and prostacyclin production. Plast Reconstr Surg 1988;81:735-41.
20. de Valence S, Tille JC, Mugnai D, Mrowczynski W, Gurny R, Moller M, et al. Long term performance of polycaprolactone vascular grafts in a rat abdominal aorta replacement model. Biomaterials 2012;33:38-47.
21. Zhang Z, Wang Z, Liu S, Kodama M. Pore size, tissue ingrowth, and endothelialization of small-diameter microporous polyurethane vascular prostheses. Biomaterials 2004;25:177-87.
22. Jeschke M, Hermanutz V, Wolf S, Koveker G. Polyurethane vascular prostheses decreases neointimal formation compared with expanded polytetrafluoroethylene. J Vasc Surg 1999;29:168-76.
23. Ahlswede KM, Williams SK. Microvascular endothelial cell sodding of 1-mm expanded polytetrafluoroethylene vascular grafts. Arterioscler Thromb 1994;14:25-31.
24. Zdanowski Z, Ribbe E, Bengmark S. Endothelialization of microporous polytetrafluoroethylene grafts in the infrarenal aorta and caval vein of the rat. Microsurgery 1992;13:277-86.
25. Hess F, Jerusalem C, Braun B, Grande P. The inner prosthetic surface structure and re-endothelialization: an experimental study in the rat using two types of microvascular prostheses for aortic implantation. Microsurgery 1986;7:29-37.
26. Robinson PH, Bartels HL, van der Lei B. Patency and healing of 10-cm long microarterial polytetrafluoroethylene prostheses in the rat abdominal aorta. J Reconstr Microsurg 1989;5:331-6.
27. Hess F, Jerusalem C, Braun B, Grande P. Patency and neointima development in 10 cm-long microvascular polyurethane prostheses implanted into the rat aorta. Thorac Cardiovasc Surg 1984;32:283-7.
28. Okoshi T, Soldani G, Goddard M, Galletti P. Very small-diameter polyurethane vascular prostheses with rapid endothelialization for coronary artery bypass grafting. J Thorac Cardiovasc Surg 1993;105:791-5.
29. Hess F, Steeghs S, Jerusalem C. Neointima formation in expanded polytetrafluoroethylene vascular grafts with different fibril lengths following implantation in the rat aorta. Microsurgery 1989;10:47-52.
30. Campbell C, Goldfarb D, Detton D, Roe R, Goldsmith K, Diethrich E. Expanded polytetrafluoro-ethylene as a small artery substitute. Trans Am Soc Artif Intern Organs 1974;20A:86-90.
31. Golden M, Hanson S, Kirkman T, Schneider P, Clowes A. Healing of polytetrafluoroethylene arterial grafts is influenced by graft porosity. J Vasc Surg 1990;11:838-44; discussion: 845.
32. Bull D, Hunter G, Holubec H, Aguirre M, Rappaport W, Putnam C. Cellular origin and rate of endothelial cell coverage of PTFE grafts. J Surg Res 1995;58:58-68.
33. Campbell GR, Turnbull G, Xiang L, Haines M, Armstrong S, Rolfe BE, et al. The peritoneal cavity as a bioreactor for tissue engineering visceral organs: bladder, uterus and vas deferens. J Tissue Eng Regen Med 2008;2:50-60.
34. Kouchi Y, Onuki Y, Wu MH, Shi Q, Ghali R, Wechezak AR, et al. Apparent blood stream origin of endothelial and smooth muscle cells in the neointima of long, impervious carotid-femoral grafts in the dog. Ann Vasc Surg 1998;12:46-54.
35. Shi Q, Wu M, Hayashida N, Wechezak A, Clowes A, Sauvage L. Proof of fallout endothelialization of impervious Dacron grafts in the aorta and inferior vena cava of the dog. J Vasc Surg 1994;20:546-56; discussion: 556-7.
36. Wu M, Shi Q, Wechezak A, Clowes A, Gordon I, Sauvage L. Definitive proof of endothelialization of a Dacron arterial prosthesis in a human being. J Vasc Surg 1995;21:862-7.
37. Branson D, Picha G, Desprez J. Expanded polytetrafluoroethylene as a microvascular graft: a study of four fibril lengths. Plast Reconstr Surg 1985;76:754-63.
38. Zacharias R, Kirkman T, Clowes A. Mechanisms of healing in synthetic grafts. J Vasc Surg 1987;6:429-36.
39. Clowes A, Kirkman T, Reidy M. Mechanisms of arterial graft healing. Rapid transmural capillary ingrowth provides a source of intimal endothelium and smooth muscle in porous PTFE prostheses. Am J Pathol 1986;123:220-30.
40. Kohler T, Stratton J, Kirkman T, Johansen K, Zierler B, Clowes A. Conventional versus high-porosity polytetrafluoroethylene grafts: clinical evaluation. Surgery 1992;112:901-7.
41. Zisch AH, Lutolf MP, Ehrbar M, Raeber GP, Rizzi SC, Davies N, et al. Cell-demanded release of VEGF from synthetic, biointeractive cell ingrowth matrices for vascularized tissue growth. FASEB J 2003;17: 2260-2.

Submitted Sep 7, 2012; accepted Nov 23, 2012.